OFFICE OF NAVAL RESEARCH

Contract No. N-00014-86-C-0808

Technical Report No. 3

VERY HIGH FREQUENCY MEASUREMENTS OF GEOMETRIC FACTORS IN TRANSMISSION LINE LEAD ACID CELLS

by

B. D. Cahan, R. R. Adzic, M. L. Daroux and E. B. Yeager

To be submitted to the

Journal of the Electrochemical Society

Case Center for Electrochemical Sciences
and the Department of Chemistry
Case Western Reserve University
Cleveland, Ohio 44106-2699

Subcontract through
The Eveready Battery Company
Westlake, Ohio 44145

15 March 1990

UNCLASSIFIED
SECURITY CLASSIFICATION OF THIS PAGE

REPORT DOCUMENTATION PAGE

1a. REPORT SECURITY CLASSIFICATION Unclassified	1b RESTRICTIVE MARKINGS
2a. SECURITY CLASSIFICATION AUTHORITY	3 DISTRIBUTION/AVAILABILITY OF REPORT Approved for public release; distribution is unlimited.
2b. DECLASSIFICATION/DOWNGRADING SCHEDULE	
4. PERFORMING ORGANIZATION REPORT NUMBER(S) Technical Report No. 3.	5 MONITORING ORGANIZATION REPORT NUMBER(S)
6a NAME OF PERFORMING ORGANIZATION Chemistry Dept. and Case Center for Electrochemical Sciences 6b OFFICE SYMBOL (If applicable)	7a NAME OF MONITORING ORGANIZATION Office of Naval Research, Chemistry Code 472
6c. ADDRESS (City, State, and ZIP Code) Case Western Reserve University Cleveland, Ohio 44106-2699	7b ADDRESS (City, State, and ZIP Code) Chemistry Program 800 N. Quincy Street, Arlington, VA 22217
8a. NAME OF FUNDING/SPONSORING ORGANIZATION Office of Naval Research 8b OFFICE SYMBOL (If applicable)	9 PROCUREMENT INSTRUMENT IDENTIFICATION NUMBER Contract No. N-00014-86-C-0808
8c. ADDRESS (City, State, and ZIP Code)	10 SOURCE OF FUNDING NUMBERS PROGRAM ELEMENT NO / PROJECT NO / TASK NO / WORK UNIT ACCESSION NO

11 TITLE (Include Security Classification)

Very High Frequency Measurements of Geometric Factors in Transmission Line Lead Acid Cells

12 PERSONAL AUTHOR(S) B. D. Cahan, R. R. Adzic, M. L. Daroux and E. B. Yeager

13a TYPE OF REPORT	13b TIME COVERED	14 DATE OF REPORT (Year, Month, Day)	15 PAGE COUNT
Interim Technical	FROM _____ TO _____	3/15/90	

16 SUPPLEMENTARY NOTATION

To be submitted to the Journal of the Electrochemical Society

17 COSATI CODES		
FIELD	GROUP	SUB-GROUP

18 SUBJECT TERMS (Continue on reverse if necessary and identify by block number)

Lead acid batteries, high frequency impedance, inductance effects

19 ABSTRACT (Continue on reverse if necessary and identify by block number)

Strip-line cells using Pb strips 1 cm wide with H_2SO_4 electrolyte have been constructed with lengths of 10 cm, 25 cm and 100 cm with several electrode spacing to test the predictions of the the theoretical models under real cell conditions. The impedance of these cells has been measured over a wide frequency range (0.1 - 10^7 Hz). New experimental techniques had to be developed for this task including the use of a new potentiostat (BC 2000) which has a full current slew rate of 4 (μs). Since the usual current measuring resistors are too inductive for use at these extreme frequencies, currents were measured with a high speed current probe (which has a bandwidth of 50 MHz). The results show clearly the effects of the inductance of the cell. These effects are clearly visible at frequencies as low as 10^2 Hz. The results suggest that the use of large battery systems in the short time domain will be seriously limited by these effects.

Research supported through a subcontract from Eveready Battery Co., Westlake, OH (prime contractor).

20 DISTRIBUTION/AVAILABILITY OF ABSTRACT	21 ABSTRACT SECURITY CLASSIFICATION
☒ UNCLASSIFIED/UNLIMITED ☒ SAME AS RPT ☐ DTIC USERS	
22a NAME OF RESPONSIBLE INDIVIDUAL Dr. Robert Nowak	22b TELEPHONE (Include Area Code) (202) 696-5075
	22c OFFICE SYMBOL

DD FORM 1473, 84 MAR — 83 APR edition may be used until exhausted. All other editions are obsolete.

SECURITY CLASSIFICATION OF THIS PAGE
UNCLASSIFIED

VERY HIGH FREQUENCY MEASUREMENTS OF GEOMETRIC FACTORS IN TRANSMISSION LINE LEAD ACID CELLS

B.D. Cahan, R.R. Adzic, M.L. Daroux

and E.B. Yeager

The Chemistry Department and

The Case Center for Electrochemical Sciences

Case Western Reserve University,

Cleveland, Ohio, 44106

ABSTRACT

Strip-line cells using Pb strips 1cm wide with H_2SO_4 electrolyte have been constructed with lengths of 10cm, 25cm, and 100cm with several electrode spacing to test the predictions of the theoretical models under real cell conditions. The impedance of these cells has been measured over a wide frequency range (0.1 - 10^7 Hz). New experimental techniques had to be developed for this task, including the use of a new potentiostat (BC 2000) which has a full current slew rate of 4A/μs. Since the usual current measuring resistors are too inductive for use at these extreme frequencies, currents were measured with a high speed current probe (which has a bandwidth of 50 MHz). The results show clearly the effects of the inductance of the cell. These effects are clearly visible at frequencies as low as 10^2 Hz. The results suggest that the use of large battery systems in the short time domain will be seriously limited by these effects.

INTRODUCTION

Only a relatively small amount of work has been published on the transient response of high power battery systems in the short time domain (0.1 μs-10ms)[1,2,3]. Most laboratory studies deal with scaled down versions of large cells that are in practice usually employed to provide standby power for applications in which continuous operation is required, rather than for pulse generation. Most recently we have reported calculations of the impedance of individual cells over a wide range of frequencies (10^2-10^8)using a modified semi-infinite strip-line model. The variables considered included the electrolyte and electrode conductivities, the electrolyte dielectric constant, the double layer capacitance, and the distributed inductance and capacitance resulting from the cell geometry. Calculation showed that the effect of various physical and geometric factors are significant at short discharge times, which can severely limit performance under these conditions[4].

In this work the measurements of the effects of physical geometry on the high frequency behavior of large power sources such as batteries have been performed at frequencies 0.1 to 10^7Hz using Pb-acid strip-line cells up to one meter long. Pronounced effects have been found for such cells which cause the effects of cell inductance to extend down to 10^2 Hz region. These effects can severely limit the performance of high power batteries in the short time domain.

EXPERIMENTAL

Cell

A glass tube 5cm in diameter sealed at the bottom was used as a cell which housed lead strip electrodes 0.5 mm thick, 10mm wide and 10, 25 or 100 cm long, mounted in Teflon holders with RTV silicone rubber (Fig. 1). Before mounting, the lead strips were polished in a mixture of glacial acetic acid and 10% H_2O_2(30%). These electrodes served as two separate working electrodes, with an auxiliary electrode external to the Teflon mounted working electrodes and a common reference electrode (SCE), (Fig. 1).

The electrolyte was 15% H_2SO_4 prepared from Fisher reagent grade acid and ultra pure water. The measurements were done with three different separations, i.e. electrolyte thicknesses, viz., 2, 4 and 8 mm. All potentials are given with respect to S.C.E.

Electronic circuitry

The electronic circuitry consisted of one BC-1200 potentiostat and one BC-2000 potentiostat of a new design. The latter has a maximum output current of $\pm$2A with a full current slew time better than 0.1 μs even with very low impedance loads. Measurements were made with a Solartron 1255 under control of an IBM CS-9000 computer. Particular care was paid to the analysis and elimination of configurational artifacts and electronic errors.

Two configurations were used for the measurements. The first

(Fig. 2) used two potentiostats and a four electrode cell. The two working electrodes (W1 and W2) were controlled against a common reference electrode (RE), with an auxiliary electrode (CE) external to the stripline cell. Balanced AC drive signals of opposite polarity were mixed with a common DC signal applied to both electrodes. In this way the cell was run such that both electrodes were at the same DC potential, but with applied AC signals of opposite polarity. The DC value could be varied over the entire Pb/PbO_2 range. The resulting impedance of the cell was thus that of two identical electrodes in series. Without this arrangement, the potential of one of the electrodes would be undefined. However, at the high frequency end of the range ($>10^3$) problems associated with current distribution between two working electrodes and the external auxiliary electrode made the measurements difficult to interpret. (In a large cell, the working electrode is <u>not</u> an equipotential surface.) It was established that the PbO_2 electrode had a sufficiently low electrochemical impedance to permit it to be used as a "non-polarizeable" counter electrode for a two electrode cell.

In the second configuration (Fig. 3), one electrode (W2 of Fig. 1) was repeatedly cycled against the counter electrode to form a thick layer of PbO_2. This served as a combined reference and counter electrode. The working electrode was charged potentiostatically against electrode AE to the PbO_2 potential. A single potentiostat then controlled the potential of WE at the desired level, starting at the most positive value. Measurements of the cell over the whole potential range could then be made after

partial reduction of the "working" electrode, since the only reaction at the PbO_2 electrode was O_2 production. At each stage, the potential of both electrodes was checked with a separate SCE reference electrode. It was essential to operate the potentiostat in the four terminal mode with separate voltage sensing (as close to the physical end of the electrode as possible) and current carrying leads to each electrode to eliminate the effects of lead resistance and inductance. Since the usual current measuring resistors are too inductive for use at these extreme frequencies, currents were measured with a Tektronix P6042 high speed current probe (which has a bandwidth of 50 MHz). In order to reduce distortion of the highest frequency measurements by the inherent phase shifts in the amplifiers of the BC-2000, voltage measurements were made using the balanced inputs of the 1255 directly. During measurements, the auxiliary electrode AE was disconnected. The physical placement of AE was sufficiently far from the working cell that perturbations of the AC current flow were negligible. The DC potential of both electrodes was monitored periodically against the reference and the potential of CE adjusted if needed by charging against AE.

RESULTS AND DISCUSSIONS

The potential dependence of impedance

Fig. 4 shows voltammetry curves of the lead electrode in 15% H_2SO_4 solution. At negative potentials in the cathodic going sweep the reduction of $PbSO_4$ takes place followed by the beginning of hydrogen evolution at even more negative potentials. In

the anodic going sweep, a large peak for the formation of $PbSO_4$ is seen. At more positive potentials the oxidation of $PbSO_4$ into PbO_2 is seen. Upon sweep reversal, the reduction of PbO_2 takes place. The impedance was measured using configuration 1 over the whole potential region from H_2 evolution to oxide formation and back from oxide formation or reduction to H_2 evolution. Configuration 2 only permitted measurement in the cathodic direction, in order to assure that the counter electrode stayed at the same state.

We can write a general expression for the impedance in polar form

$$Z = x + iy = |Z| e^{i\theta} \qquad (1)$$

or in terms of logarithms,

$$\log Z = \log |Z| + i\theta \qquad (2)$$

where $Z = (x^2 + y^2)$ and $\theta = \tan^{-1}(Y/X)$, as the principal value so as to define log Z as a single valued function.

The plot of log $|Z|$ and θ vs. log f is called a Bode plot in which the impedances of all ideal components are represented by simple straight lines. The slope of a "pure" resistor is zero (with a phase angle of zero), of a "pure" capacitor is -1 (with a phase angle of -90°) and the slope of an inductance is +1 (with a phase angle of +90°).

Figures 5-7 display the Bode plots of the impedance and the phase angle of the Pb/H_2SO_4 electrode (25 cm) in four different

potential regions as a function of frequency. These potential regions correspond to the impedance of bare Pb, including H_2 evolution (5a); oxidation of Pb into $PbSO_4$ (5b); of $PbSO_4$ layer (6a) and the oxidation of $PbSO_4$ into PbO_2 (6b). Figures 7a and 7b show the plots for PbO_2 and the reduction of PbO_2 into $PbSO_4$.

A close inspection of the curves in Fig. 5a shows that for several potentials the impedance plots have a slope of -.9 (close to -1) with a corresponding phase angle of 80-83° over a significant portion of the frequency range. This is indicative of the predominantly capacitive behavior* of the lead electrode in this potential region in H_2SO_4. The slope is not identically -1, since the cell is behaving partially as a transmission line**. The curves at the lowest potentials which correspond to the onset of H_2 production (such as curves 1 and 2) deviate from this slope at lower frequencies due to this faradaic reaction. The decrease of the phase angle of curves 1 through 6 at the lowest frequencies shows that this reaction is occurring at these potentials, also, although at much lower rates, and would have been evident at

---

*. The value of this capacitance measured at 1000 Hz is approximately 1670 μF, or 67 $\mu F/cm^2$. This value should not be taken too literally, as the distributed nature of the cell affects it.

**.In complex plane terms, this would be called a "constant phase element". This would however hide the true nature of the distributed impedance.

frequencies well below 1 Hz*. The small potential dependence of the impedance plots in the frequency range up to $\approx 10^3$ Hz in curve 3-8 is probably due to the reduction of residual patches of $PbSO_4$ as the potential is shifted to more negative values.

At frequencies higher than 10^3 Hz the slope becomes almost zero. This is a measure of the resistive behavior of the electrolyte (see below). At even higher frequencies (10^5), the slope assumes positive values, as the system becomes inductive. This is a real physical inductance, caused by the loop formed as the current travels down one electrode, through the solution, and back up the other side. This inductance is also a distributed system, and the phase angle is not +90°. As pointed out above, in this region of frequencies the current distribution problems between the two electrodes affected these measurements. These data clearly show that the electrode physical geometry can generate impedance components which are detrimental to the performance of large batteries at short times.

Fig. 5b shows the plots of impedance and phase angle for several potentials in the Pb -->$PbSO_4$ reaction range. Curve 1 shows the impedance at the very beginning of the formation proc-

---

*. An interesting artifact is observable in curve 1. The impedance rises between 1 and 10 Hz. This would normally be interpreted as "inductive" behavior, but the corresponding phase angle plot clearly goes to zero. The phase angle is thus that of a resistor. However, these measurements were done with frequencies increasing, and at this potential, H_2 bubbles gradually accumulate, partially blocking the surface, and increasing the resistance of the surface with time. This is a good example of the necessity of the use of phase angle measurements when interpreting impedance data.

ess. Note that the slope is very close to -0.5, rather than 1. This value can be associated with the behavior of an RC transmission line. It can also be interpreted as the result of a progressive formation of a thin layer down the gap as oxidation proceeds slowly. It is probably not caused by local heterogeneity of the surface. At these frequencies, the measured capacitance of a heterogeneous surface should be the simple geometric average of the local values. At the potential of curve 2, the electrode appears more uniformly co· ·ed with a thin layer of $PbSO_4$.* As oxidation continues, the impedance increases considerably as more $PbSO_4$ is formed on the surface. At lower frequencies, for several potentials, the slope is close to zero because of the effects of the reaction resistance, the value of which increases as the surface coverage becomes thicker and more dense. For the most positive potentials in this plot the impedance plot again shows a slope close to -1, i.e. the capacitance of the lead surface covered by $PbSO_4$ determines the behavior . The impedance of this electrode is approximately one order of magnitude larger than that of Pb electrode. As for Fig. 5a, the phase angle is in agreement with the features of the impedance plot.

Fig. 6a shows the plots in the potential region in which the surface coverage by sulfate is increasing. The impedance varies somewhat with applied potential as the film thickens**. As in Fig.

---

*. An artifact similar to the one observed for H_2 blocking is observed.

**. The capacitance varies from a high of 66μF (or 2.64$\mu F/cm^2$ for curve 3 of Fig. 5b to a value of 16.7μF (or 0.67$\mu F/cm^2$ for curve 8 of Fig. 6a.

5b, the slope is close to -1 and it extends up to 10^5Hz.

Fig. 6b displays the plots obtained in the potential region of $PbSO_4$ --> PbO_2 reaction. As the conductive oxide replaces the non conductive sulfate on the surface the impedance decreases considerably, reaching at the most positive potentials approximately three orders of magnitude lower values. At frequencies $>10^2$ Hz, the resistance determines electrode's impedance, as evidenced by a slope close to zero*. Considering the high conductivity of lead dioxide it appears that this resistance is due to the electrolyte. The phase angle changes according to the changes of the impedance. It is close to zero in the frequency/potential region in which the resistive impedance dominates.

Fig. 7a shows the plots for the reduction of lead dioxide into lead sulfate. An increase of impedance is seen which, with a shift of potential in negative direction, gradually approaches the values close to the ones for a large coverage of sulfate (Fig. 7b).

The effects of the length of electrode

The effects of the length of electrode have been studied

---

*. The resistance of the electrolyte varies from 0.034 ohms at 100 Hz to 0.028 ohms at 10000 Hz, corresponding to an average resistiviy of 2.12 to 1.75 ohm-cm. Note that the effective resistance decreases slightly with increasing frequency. This behavior was not expected, since the penetration depth shold decrease with increasing frequency, thus raising the effective electrolyte resistance.

with the electrodes of .1, .25 and 1m in length. Fig. 8 shows the data obtained in the potential range for which the surface is covered by lead sulfate. The same conclusions regarding the electrode length could be obtained at all potentials used. Two limiting cases of the impedance control are seen in Fig. 8. In the lower frequency region, an RC circuit is an electrical analog of the electrode behavior, causing the slope of the log Z vs. log w to have a value of -1. Depending on the length of the electrode, the circuit reduces to an RL network with the above slope approximately equal to +1. Fig. 8 shows that the frequency at which the change of slope takes place shifts to lower values with increasing the length of the electrode. This is a clear indication of the limitations of the applications of large batteries for discharge at high frequencies. It is likely that in the presence of faradaic reactions, such as those that occur during the discharge of battery, this characteristic frequency is probably lower than the values for $PbSO_4$ given in Fig. 8.

The effects of the thickness of electrolyte

The separation of electrodes, i.e. the thickness of the electrolyte layer in the strip-line cell is visibly affecting the impedance of the cell. Fig. 9 displays the data for the cell one meter long with the electrolyte layer 2, 4 and 8mm thick. It is seen that the changes of the resistance of the cell are not pronounced on the logarithmic scale. The effect of electrode separation on the inductance is clearly seen. The effects of inductance are observed at lower frequencies with increasing of the electrode separation. It shifts from approximately 10^5 Hz,

for the 2 mm separation, to approximately 10^4 Hz for 8 mm thick electrolyte layer. This is to be expected for increased separation, since it causes the inductive loops to increase too. The data corroborates the previous conclusion regarding the effect of physical geometry of the cell, based on the data for various lengths of electrodes.

IR-corrected impedance plots

In the second measuring configuration with one potentiostat, the new BC2000 whose wide bandwidth, coupled with the use of the Solartron 1255, permitted measurements from 0.1 Hz to up to 10^7 Hz. To our knowledge this is the first time reliable impedances have been measured over as wide a frequency range. The precision of these measurements was such that IR correction was possible down to the milliohm level.

In these measurements, the electrode served also as a reference. Both, working and counter electrodes were carefully charged to eliminate any $PbSO_4$ films. The measurements were done with 10 and 100 cm long cells to compare the effects of inductances of sizable difference on the cell impedance. Fig.10 shows the plots for 10 cm long PbO_2 electrode undergoing a partial reduction to $PbSO_4$. The capacitive behavior of the impedance is seen up to 10^2 Hz for several potentials. Due to a small length of the electrode, the effect of inductance for a given cell is shifted to 10^5 Hz. As shown for the electrode of 25 cm in length, the formation of $PbSO_4$ causes an increase of impedance and the phase angle

reflects the changes in impedance. At very low frequencies, i.e. <1 Hz, a resistive behavior of the impedance is seen, probably caused by the reaction resistance. Consequently, the phase angle assumes the values close to zero. Fig. 11 shows the plots for further reduction of PbO_2 into $PbSO_4$ at more negative potentials. Further increase of the impedance is seen as more compact layer $PbSO_4$ has formed.

Figures 12 and 13 show the data for impedance of 1m long cell. The manifestation of the cell inductance occurs at lower frequencies than for .1m cell. Curves 1) and 2) show capacitive and resistive behavior up to 10^4 Hz after which point the cell appears almost completely inductive. At more negative potentials, a partial film of $PbSO_4$ begins to block the surface. The stability and precision of these measurements was such that the series resistance (of the electrode and of the electrolyte) could be subtracted, leaving the curves of Fig. 13. From these curves it can be seen that the effects of the cell inductance extends down to the 100 Hz region. This is an important finding. The inductance in battery systems occurs at relatively low frequencies, but it is not seen in the measurements without IR correction because of the dominating resistive behavior up to 10 - 10^5 Hz.

The above data clearly show the effects of the cell physical parameters on the cell impedance. In particular important appears the evidence for inductive behavior of the lead-acid cell already at relatively small dimension, and at relatively low frequencies (10^2 - 10^4 Hz). It can be concluded therefore that the use of large battery systems in the short time domain will be seriously limited. Besides this, the paper brings the most complete meas-

urements of the impedance of a lead electrode in sulfuric acid solution in the whole potential range from .1 Hz to 10^7 Hz.

Acknowledgements

Financial support of the Office of Naval Research is fully acknowledged.

REFERENCES

(1)P.L. Kapitza, Proc. Roy. Soc. Lond. **105a**,691, (1924)

(2)J.J. Lander,E.E. Nelson, J. Electrochem. Soc., **107**, 722 (1960)

(3)R.M. LaFollette, D.N. Bennion; 171st ECS Meeting Extended Abstracts, 87-1, p40 Abs No. 29, Philadelphia, (May 1987) and references therein.

(4)B.D. Cahan, M.L. Daroux and E.B. Yeager, J. Electrochemical. Soc., **136**, 1585, (1989).

List of Figures

4, 4') 1.4V; 5, 5') 1.4V; 6, 6') 1.3V; 7, 7') 1.2V; 8, 8') 1.1V (A). 1 to 8 and 1' to 8') 1V to .3V (decrements:.1V) (B).

Fig. 8 Impedance plots of 10, 25 and 100 cm long Pb strip-line cell in 15 % H_2SO_4 with a layer of $PbSO_4$ on the surface. Potential range from .1V to 1.2V.

Fig. 9 Impedance and phase angle plots of an 100 cm long Pb strip-line cell in 15 % H_2SO_4 as a function of potential. The electrode separations : 2mm(a), 4mm(b), and 10 mm(c).Electrode potentials: the curves 1) to 8) and 1') to 8') 1.1V to 1.8V.

Fig. 10 Impedance and phase angle plots of an 10 cm long Pb strip-line cell in 15 % H_2SO_4.The curves 1) to 8) 0V to .7V. (increment:.1V).

Fig. 11 Impedance and phase angle plots of an 10 cm long Pb strip-line cell in 15 % H_2SO_4.The curves 1') to 5') .8V to 1.2V.(increment:.1V).

Fig. 12 Impedance plots of an 100 cm long Pb strip-line cell in 15 % H_2SO_4. The curves were measured at: 1) 2.2 V; 2) 2.15 V; 3) 2.1 V; 4) 2.05 V; 5) 2.0 V; 6) 1.95 V.

Fig. 13 Impedance plots of an 100 cm long Pb strip-line cell in 15 % H_2SO_4. The data from Fig. 12 after subtraction of a resistance of 50 mΩ.

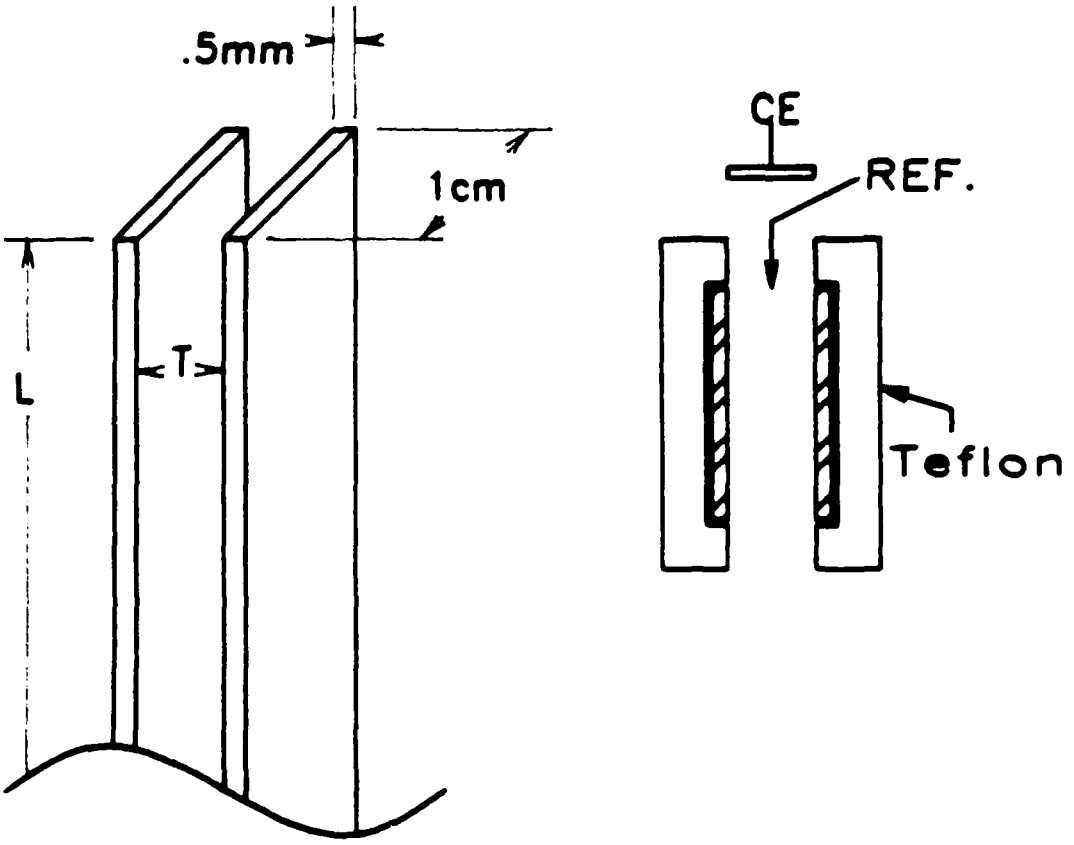

Fig. 1 Schematic drawing of the strip-line cell

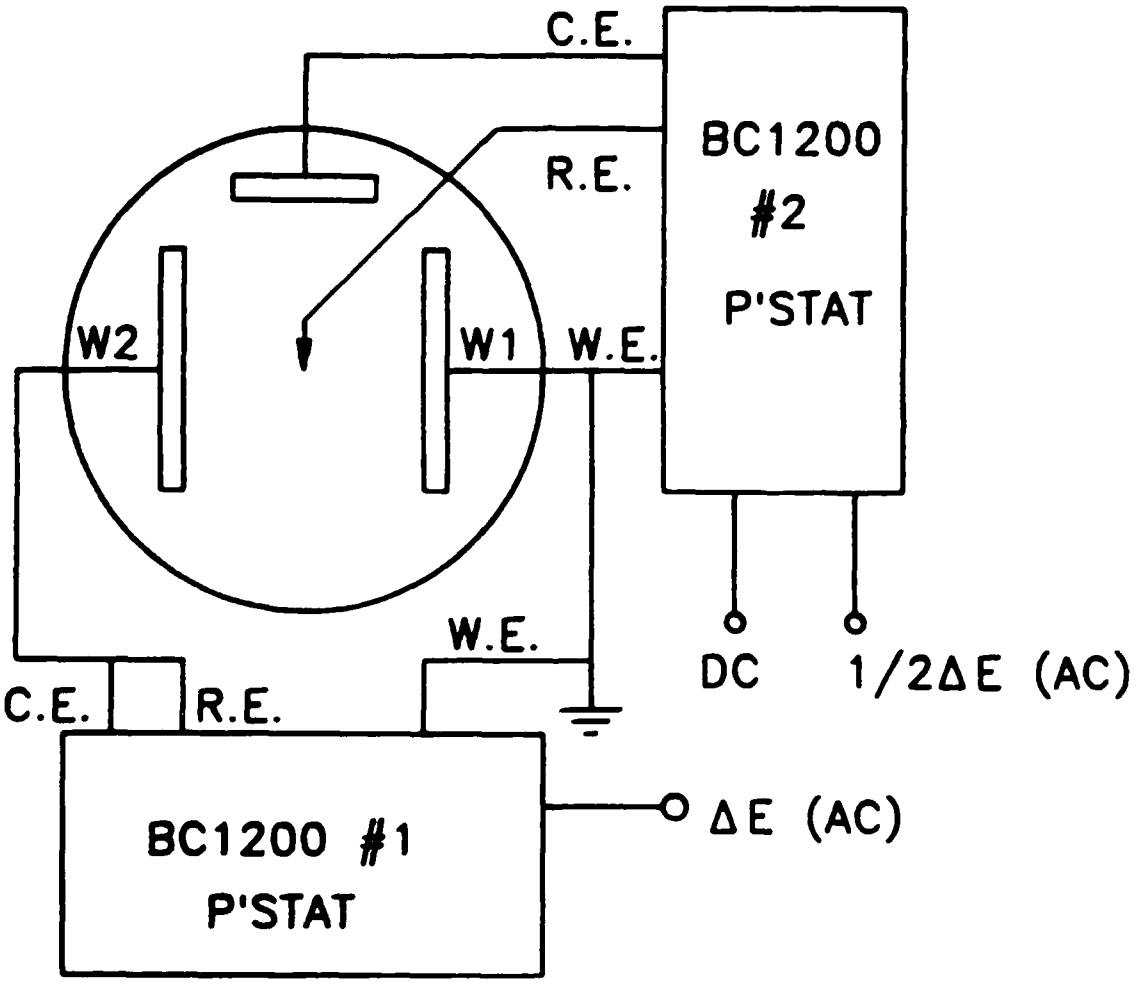

Fig. 2 Schematics of the two potentiostat configuration and a four electrode cell. Solartron 1255 not shown.

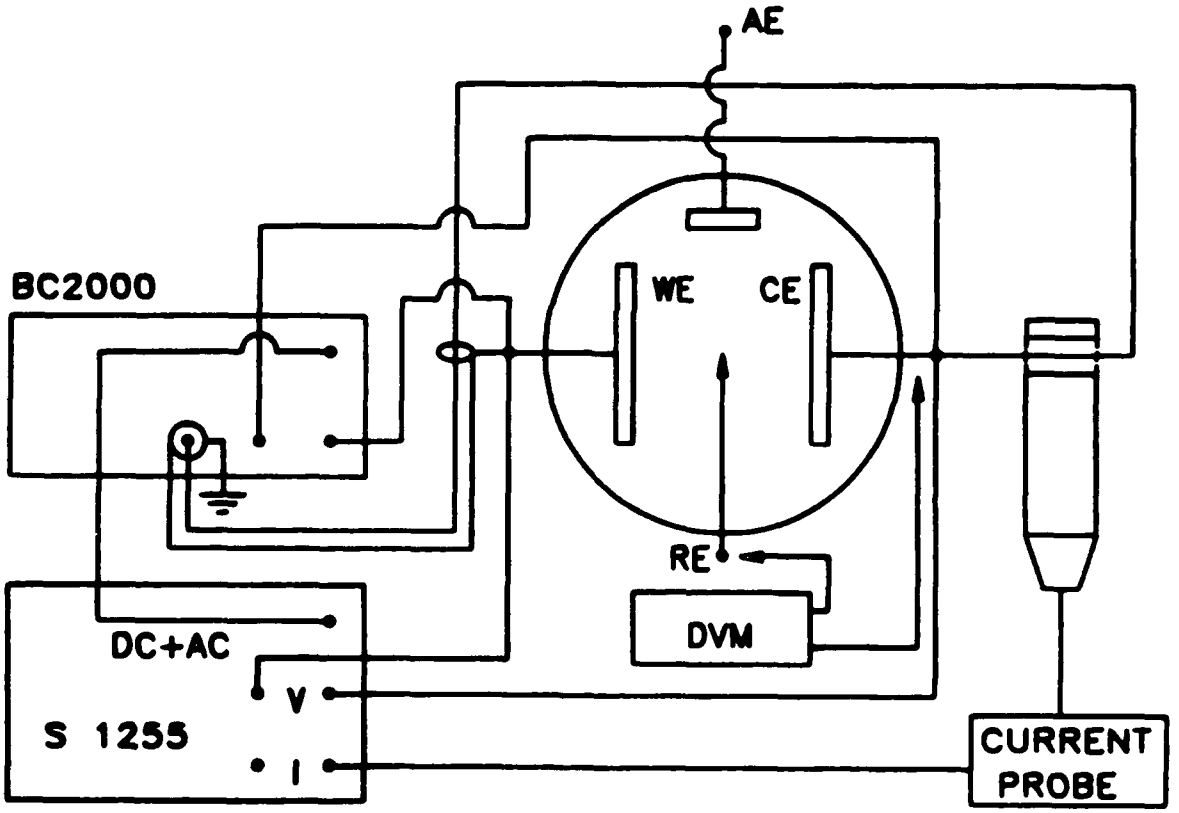

Fig. 3 Schematics of the measuring circuit with a single potentiostat.

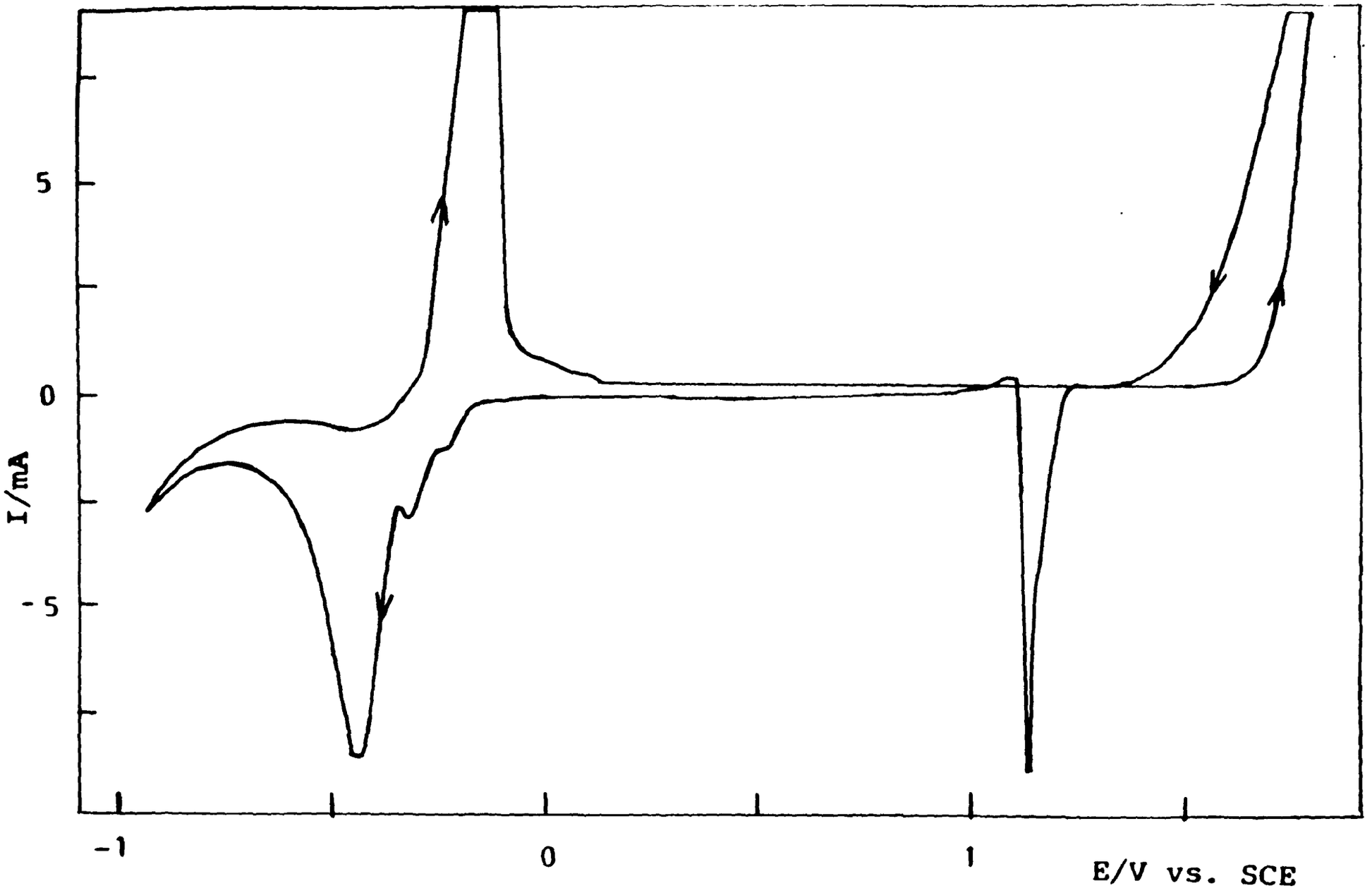

Fig. 4 Voltammetry curve for a lead electrode in 15 % H_2SO_4.

Sweep rate : 20 mV/s.

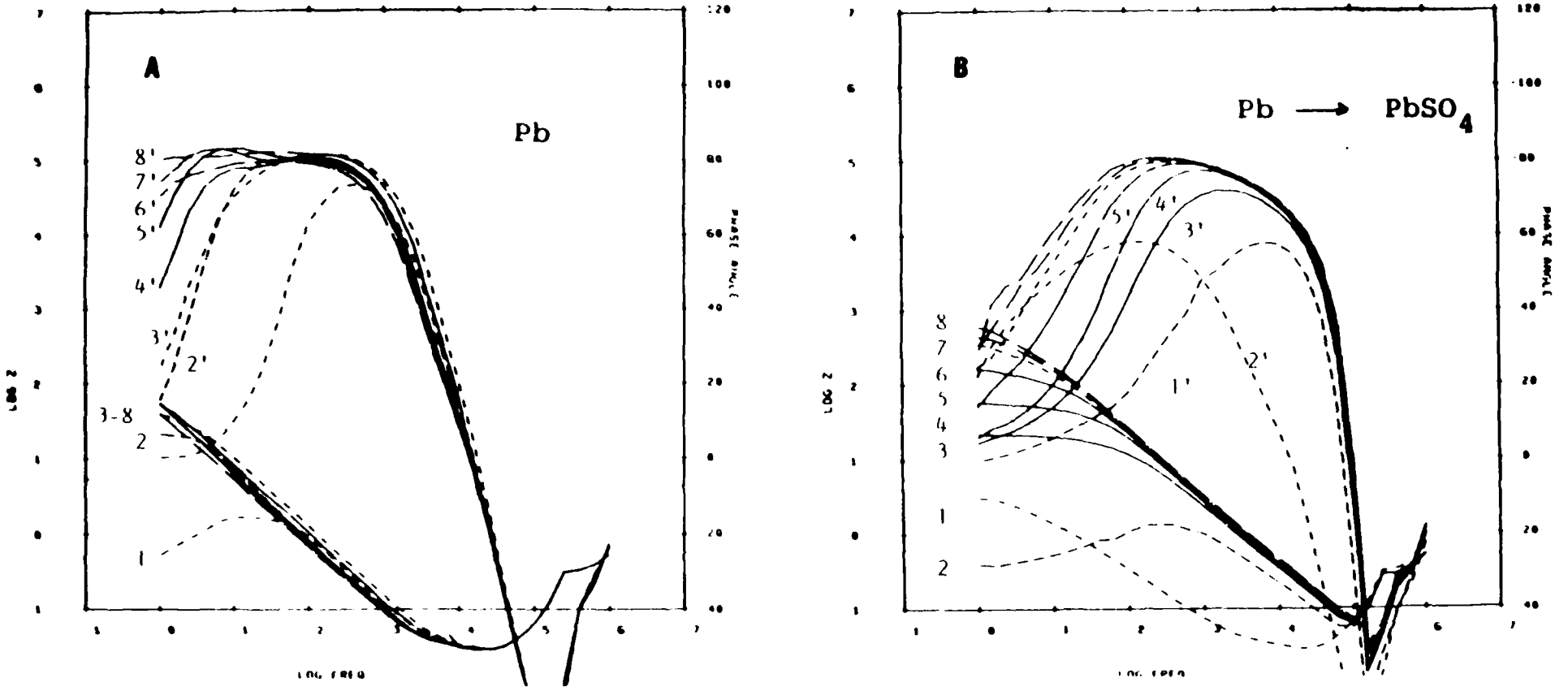

Fig. 5 Impedance and phase angle plots of an 25 cm long Pb strip-line cell in 15 % H_2SO_4. Numbers correspond to the following electrode potentials : 1, 1') -.6V SCE; 2, 2') -.7V; 3, 3') -.8V; 4, 4') -.9V; 5, 5') -1V; 6, 6') -1.2V; 7, 7') -.7V (in anodic direction); 8, 8') -.6V (A) and 1, 1') -.55V; 2, 2') -.5V; 3, 3'), -.4V; 4, 4') -.3V; 5, 5') -.2V; 6, 6'-.1V; 7, 7) .0V; 8, 8') .1V (B).

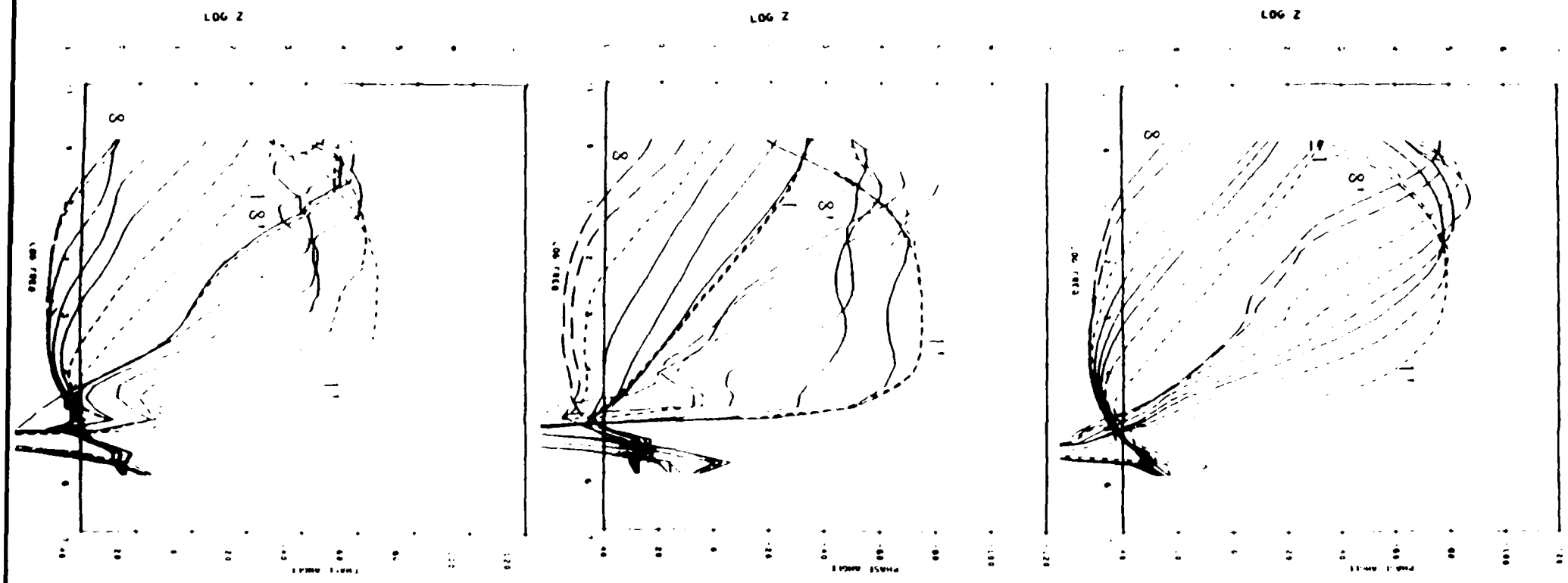

Fig. 9 Impedance and phase angle plots of an 100 cm long Pb strip-line cell in 15 % H_2SO_4 as a function of potential. The electrode separations : 2mm(a), 4mm(b), and 10 mm(c).Electrode potentials: the curves 1) to 8) and 1') to 8') 1.1V to 1.8V.

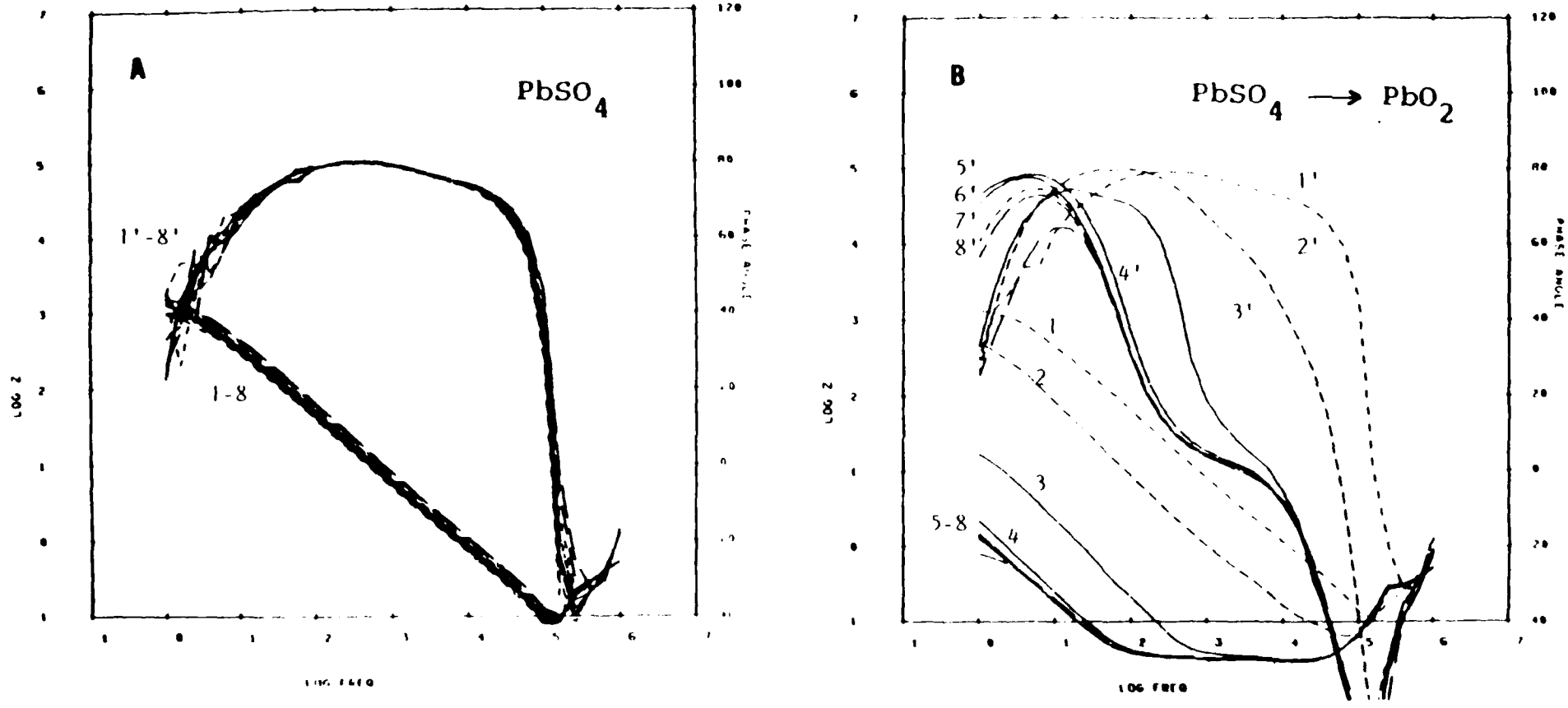

Fig. 6 Impedance and phase angle plots of an 25 cm long Pb strip-line cell in 15 % H_2SO_4. Numbers correspond to the following electrode potentials : 1) to 8) .2V to 1.3V (increments: .1V or .2V) (A) and 1') 1.5V; 2') 1.6V; 3' 1.65V; 4') 1.7V; 5') 1.75V; 6') 1.8V; 7') 1.9V; 8') 1.8V.

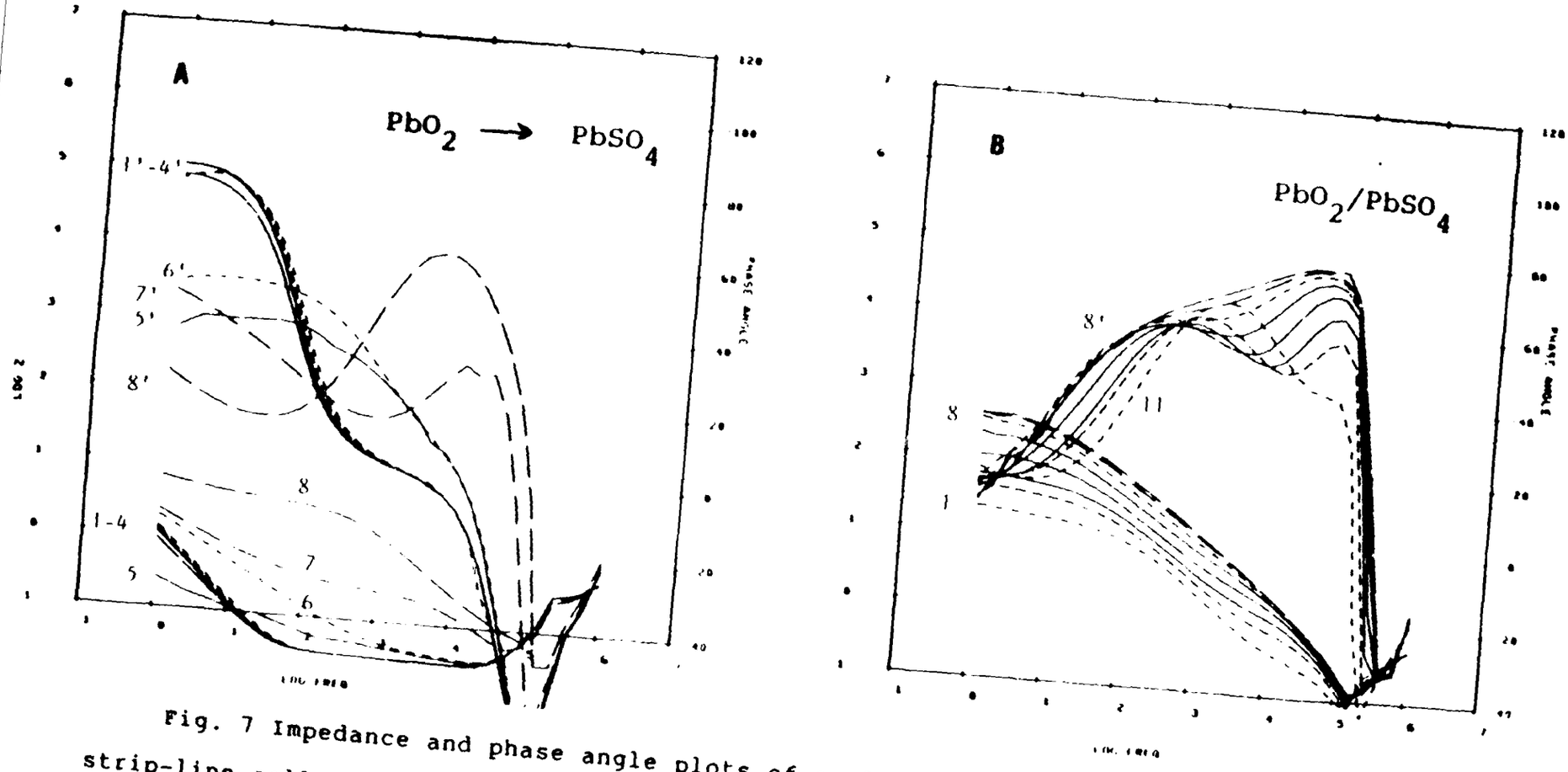

Fig. 7 Impedance and phase angle plots of an 25 cm long Pb strip-line cell in 15 % H_2SO_4. Numbers correspond to the following electrode potentials : 1, 1') 1.7V; 2, 2') 1.6V; 3, 3') 1.5V; 4, 4') 1.4V; 5, 5') 1.4V; 6, 6') 1.3V; 7, 7') 1.2V; 8, 8') 1.1V (A). 1 to 8 and 1' to 8') 1V to .3V (decrements:.1V) (B).

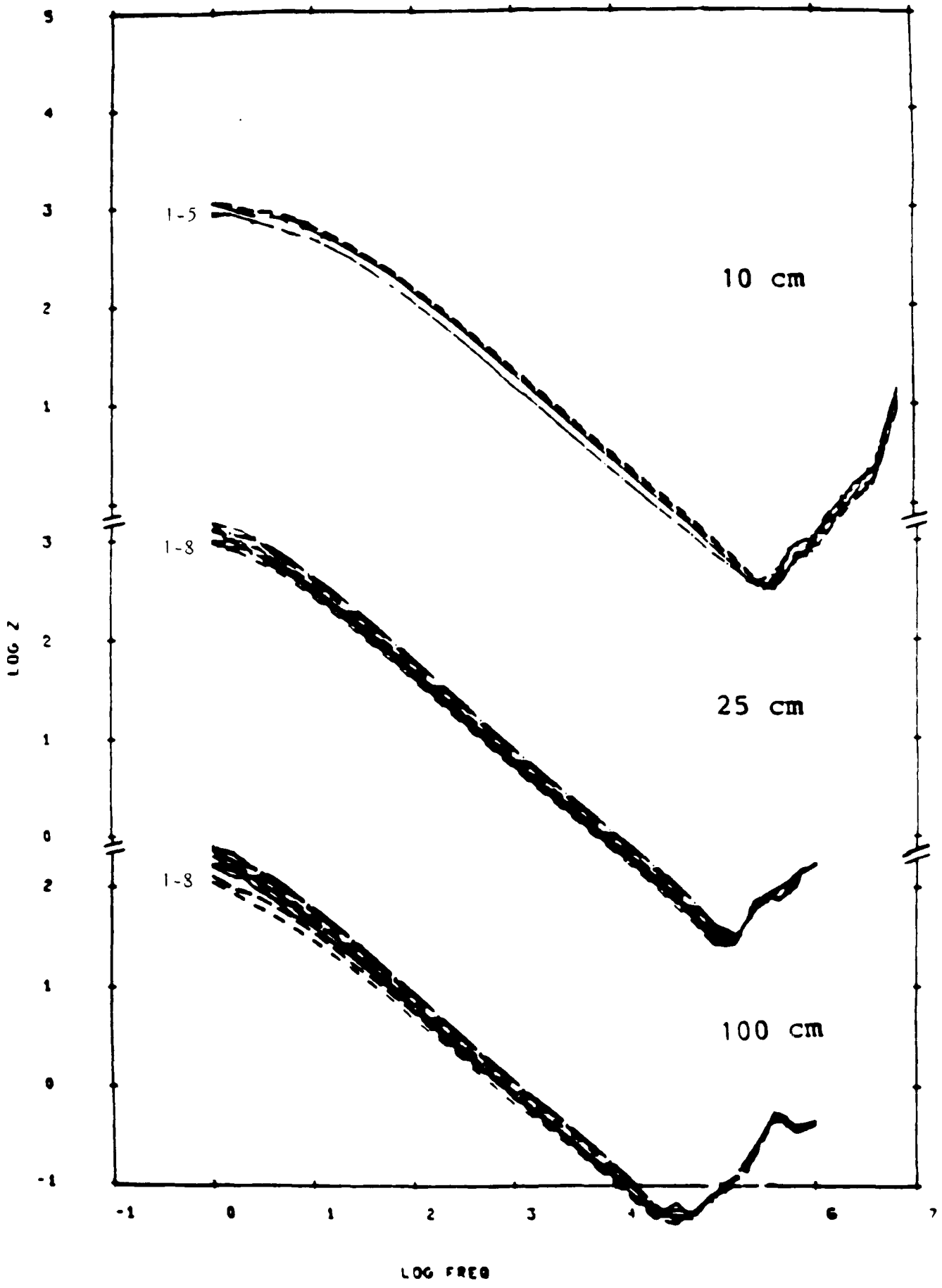

Fig. 8 Impedance plots of 10, 25 and 100 cm long Pb strip-line cell in 15 % H_2SO_4 with a layer of $PbSO_4$ on the surface. Potential range from .1V to 1.2V.

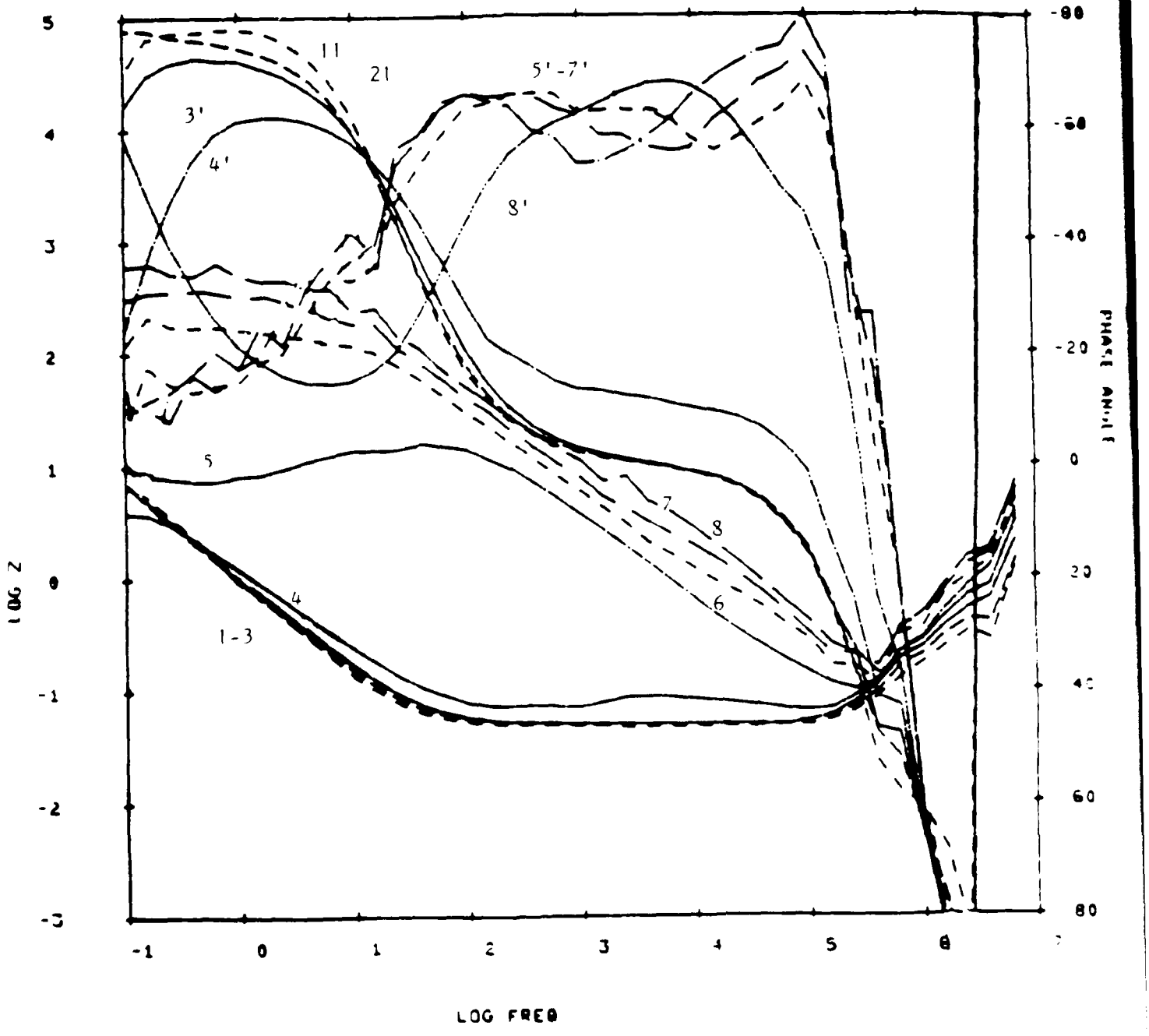

Fig. 10 Impedance and phase angle plots of an 10 cm long Pb strip-line cell in 15 % H_2SO_4.The curves 1) to 8) 0V to .7V. (increment:.1V).

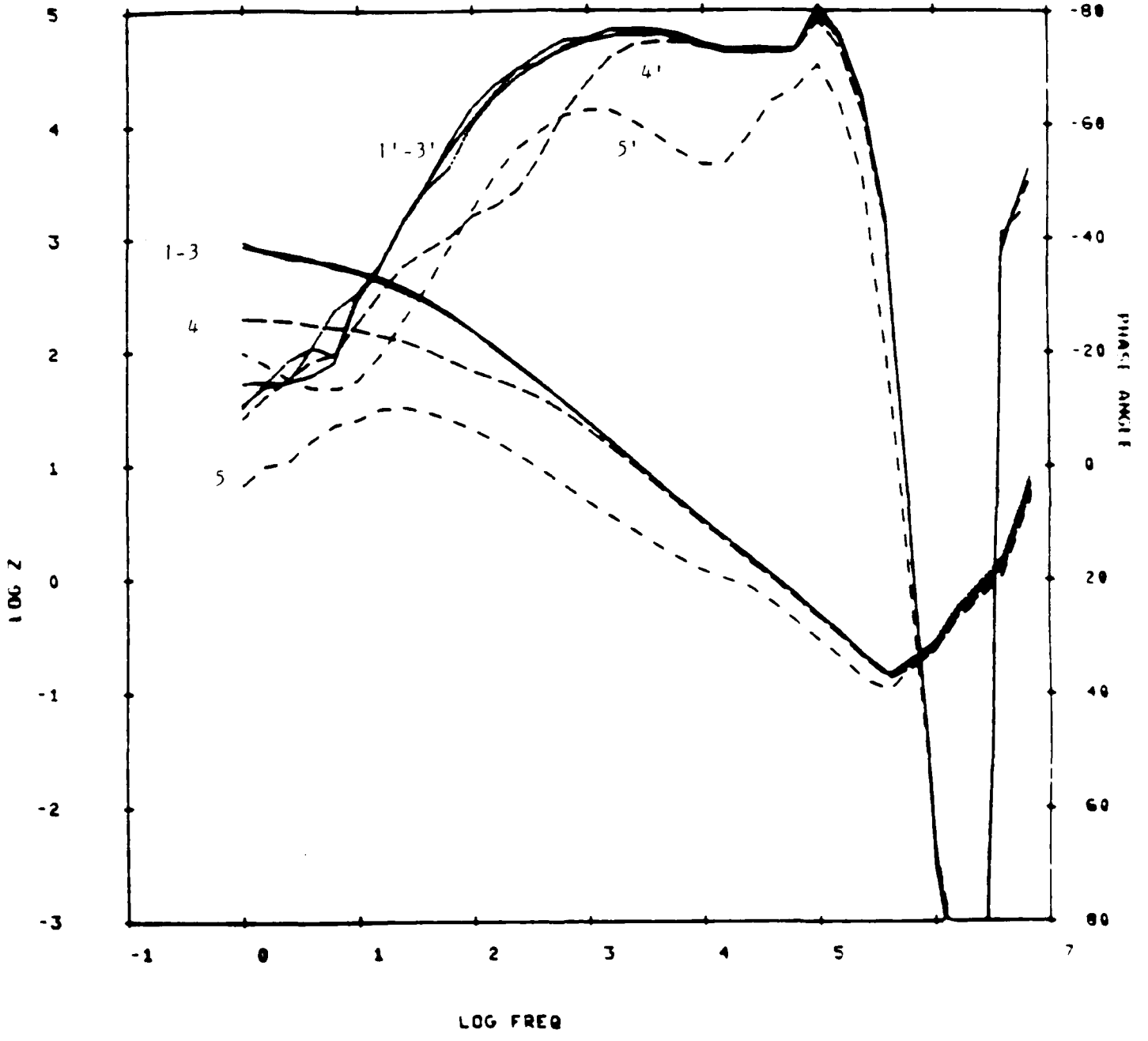

Fig. 11 Impedance and phase angle plots of an 10 cm long Pb strip-line cell in 15 % H_2SO_4.The curves 1') to 5') .8V to 1.2V.(increment:.1V).

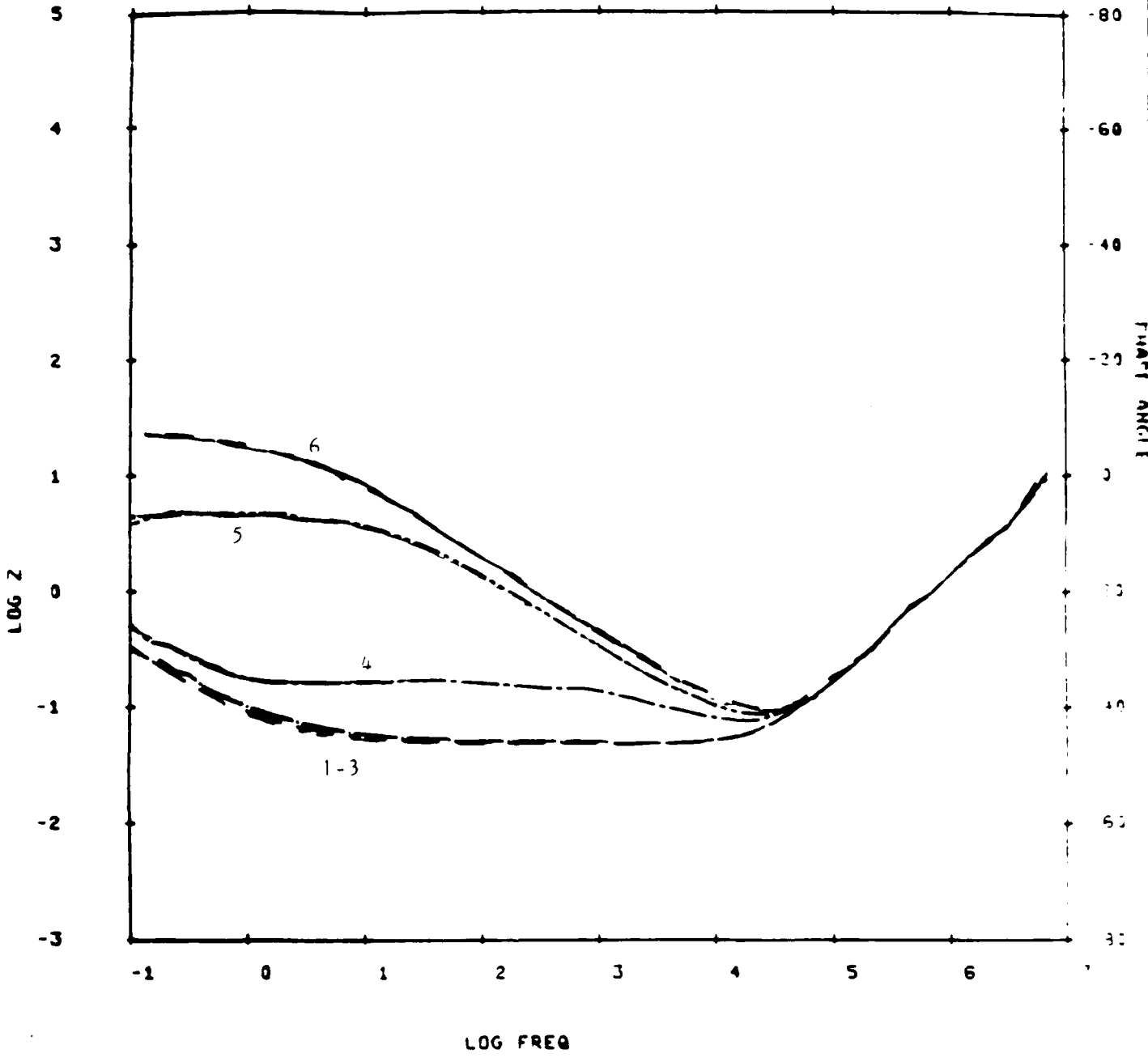

Fig. 12 Impedance plots of an 100 cm long Pb strip-line cell in 15 % H_2SO_4. The curves were measured at: 1) 2.2 V; 2) 2.15 V; 3) 2.1 V; 4) 2.05 V; 5) 2.0 V; 6) 1.95 V.

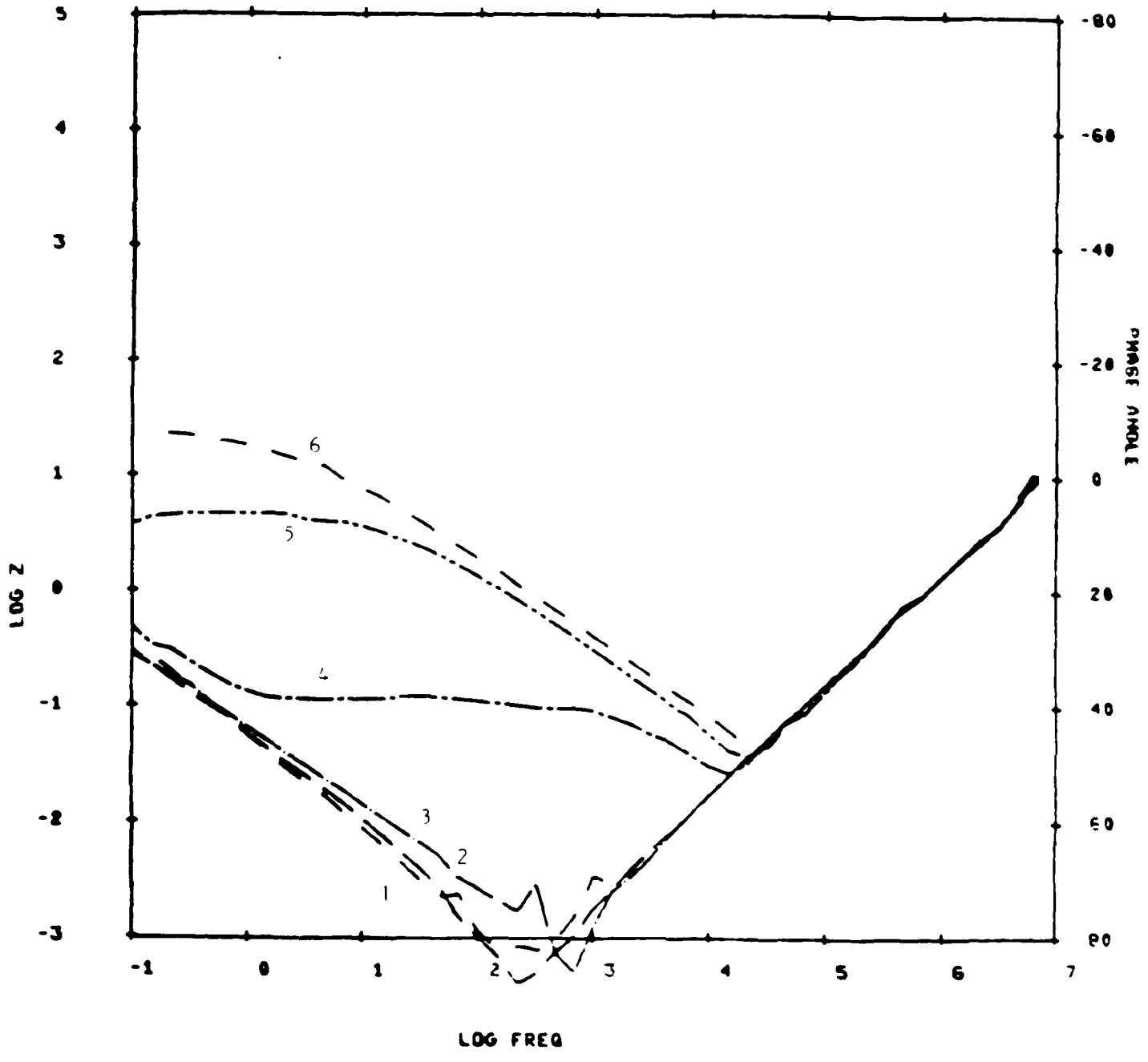

Fig. 13 Impedance plots of an 100 cm long Pb strip-line cell in 15 % H_2SO_4. The data from Fig. 12 after subtraction of a resistance of 50 mΩ.